EXPERIMENT TO MEASURE THE ELECTRON CLOUD AT BEPC*

Z.Y. Guo, Q. Qin, J.S. Cao, H. Huang, L. Ma, J.Q. Wang, J. Xing, G. Xu, C. Zhang, Z. Zhao,
Institute of High Energy Physics, Chinese Academy of Sciences, Beijing, 100039, P.R. China,
K.C. Harkay, Argonne National Laboratory, Argonne, IL 60439, USA, H. Fukuma, E. Kikutani,
M. Tejima, High Energy Accelerator Research Organization, 1-1 Oho, Tsukuba, Ibaraki, 305, Japan

1 INTRODUCTION

Many experiments on photoelectron instability (PEI) have been carried out at the Beijing Electron Positron Collider (BEPC) in IHEP, China, in collaboration with KEK[1]. Simulations on the PEI with a physical model give qualitative agreements with the observations at both BEPC and KEK-B. Based on the detectors at Advanced Photon Source (APS), ANL, a specially-constructed detector was installed at the BEPC. It is hoped to obtain realistic values for the photoelectron (PE) and secondary electron yields as well as the energy spectrum of the electron cloud through the direct measurements of the properties of the PE cloud for both stable and unstable beams. In this paper, the experimental results at the BEPC are presented after the description of the instrumentation, and some discussions are followed afterwards.

2 INSTRUMENTATION

2.1 The PE detector

Similar to the detector in APS[2,3], we made a photoelectron detector, which has three layers with the same diameter of 80 mm. Two mesh grids are in front of the detector. The outermost grid is grounded, and a bias voltage is applied to the shielded grid. The collector is graphite-coated to lower the secondary electron yield and is biased with a DC voltage of +48 V with batteries. The whole detector was mounted on an idle profile slot, whose diameter is 100 mm located on the top of the vacuum chamber. There is a 1-cm annular gap between the detector and the support barrel.

Unlike that in the APS, the BEPC detector is mounted downstream of a bending magnet in the direction of positron motion, shown in Fig. 1, with a distance of 230 mm between the dipole and the detector.

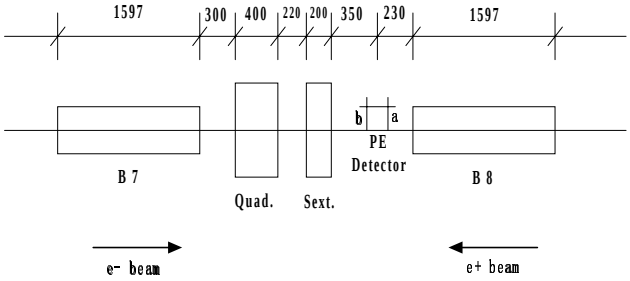

Figure 1: Position of the PE detector at the BEPC storage ring (seen from inside of the ring).

*Work supported by the Chinese National Foundation of Natural Sciences, contracts 19875063-A050501 and 19975056-A050501

Being so close to the dipole, the PE detector has to be shielded from the magnetic field with layers of high and low permeability "mu-metal" sheets and nickel alloy sheets. After shielding, the fields at the points *a* and *b* in Fig. 1 are 9 Gauss and 0, respectively. At the centre inside the detector chamber, the fringe field of the dipole is measured using a model chamber installed in a reference dipole, which has the same field of the dipoles in the storage ring. The result confirms the effect of shielding.

2.2 Apparatus setup

Shown as Fig. 2, the collector is first connected in series with the batteries, then a low pass filter (LPF) is linked to verify that the collector signal is due to the electron only and to see if there is any influence from the RF noise. With the LPF, a 0.1 MΩ resistor is connected, which can be used to check the direction of the current from the collector, using a voltmeter connected across the resistor. The nanoammeter, which is connected between the resistor and ground to measure the current of photoelectron, can be cross-checked with the readings of the voltmeter. A temperature monitor is mounted on the detector to detect heat induced by beam-excited HOM wakefields in the annular gap between the detector and the support barrel.

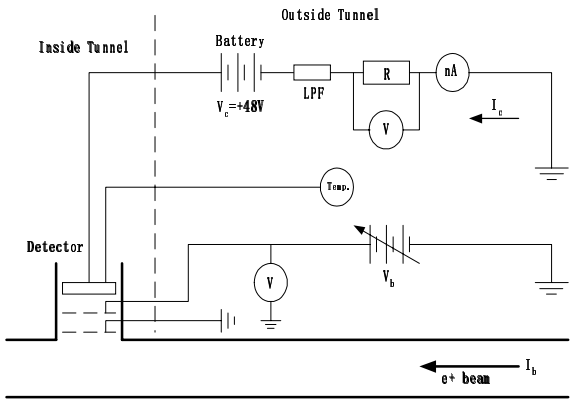

Figure 2: Setup of all apparatus used in the experiment

3 MEASUREMENTS

3.1 Instrumentation check with beam

In order to filter the beam-induced RF noise, an LPF is used in the experiment. With different LPF cutoff frequencies, we measured the detector current (I_c) as a function of beam current, shown as Fig. 3.

In a series of measurements, , we acquired a number of curves without the LPF, as shown in the left plot of Fig. 3, and in the right plot similar curves with the LPF are

shown. So, for further PE measurements, we apply the 150 MHz LPF to eliminate any sources of noise.

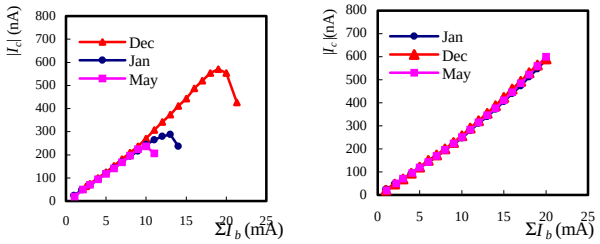

Figure 3: Effect of LPF.
(Left: without LPF, Right: with 150 MHz LPF)

During all the measurement, the temperature monitor displays 24±1°C with no change, which means the HOMs effect due to the annular gap between the detector and its support barrel is minimal. All these confirm the validity of the whole measurement system. A bias voltage scan was made and the V_b fixed at +40V for maximum signal, as shown in Fig. 4. It can be seen that electron beam creates a PE signal that is about 6 times lower than with positron beam. One reason the curve of positron beam is higher than that of electron beam is that the detector is located 6 times closer to the downstream dipole (B8) for the positron beam, than the distance from the detector to the downstream dipole (B7) for the electron beam, as shown in Fig. 1. Another reason may be that the interaction of the PE with the positron beam may cause more electrons to be deflected into the detector. So positron beam is used in the following measurements.

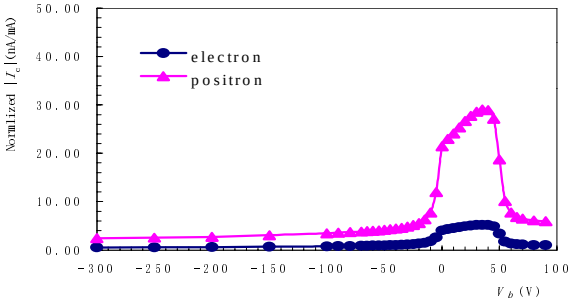

Figure 4: Detector current when bias voltage scans.

3.2 Dependence on beam current

The collected electron current I_c as a function of beam current I_b is measured in the cases of single bunch and multi-bunch. The linear curves of this relation are obtained similarly to the curves shown in the right plot of Fig. 3. Normalized by I_b, I_c is almost the same in different beam conditions with a constant about 25nA/mA.

We try to look for the saturation effect, in which the processes of electron generation and loss equilibrate, with a long bunch train and a weak bunch current. But no any saturation process of electron collection is found even extending the bunch number to 40 with the bunch current of 1 or 2 mA (the beam current is 40 or 80 mA). The reason might come from the fact that the detector is located very near the dipole and there is no antechamber, causing the primary photoelectron emission to dominate over secondary electron emission .

The derivative of the normalized I_c-V_b curve gives the photoelectron energy distribution, shown as Fig. 5.

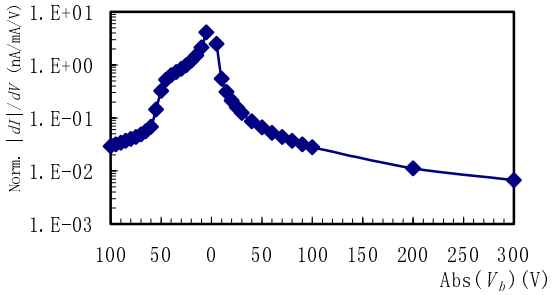

Figure 5: Photoelectron energy distribution.

With an oscilloscope, the time structure of the I_c can be directly observed. The signal on the oscilloscope looks suspicious since the noise might be too strong. A possible way to observe it would be amplifying the signal near the detector using a 600 MHz LPF to attenuate high frequency HOMs.

3.3 Secondary electron (SE) measurement

Due to the SE, a dramatic amplification of the signal is observed in the APS when the bunch spacing is 7 buckets (20 ns) [2]. The energy gain of the electrons kicked by the beam is determined by $\Delta p = 2m_e N_b r_e c/a$, where a is the radial distance from the beam and r_e the classical electron radius. Compared with the APS case, the beam-induced multipacting may be expected to appear on 5-bucket spacing and 6 mA/bunch in the case of BEPC. But in our measurement, such amplification is not obtained when the bunch spacing and current are scanned from 1 mA/bunch to 6 mA/bunch with the bunch spacing from 1 to 12 buckets in a bunch train of 5 and 10 bunches, shown in Fig. 6. The only result is the normalized electron current increases when increasing the bunch current. The possible reason may come from the short distance between the bending magnet and the detector, which may cause the photoelectrons to dominate and possibly suppress the secondary electrons.

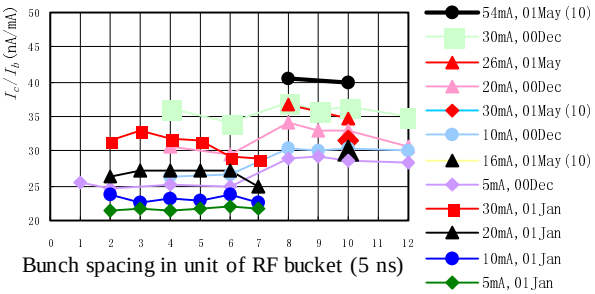

Figure 6: Normalized electron current as a function of bunch spacing and current.

3.4 Dependence on beam parameters

In the experiment, we measure the I_c as functions of beam parameters. The correlations were measured with different beam closed orbit, beam energy, beam emittance and chromaticity, respectively. The dependence of I_c on beam energy, emittance and chromaticity are not sensitive

when keeping the closed orbit fixed. With an I_b of 1 mA, the I_c has 1 nA linear increment when the vertical closed orbit increases 1 mm. This indicates the PE distribution is quite sensitive to the beam position.

A kind of vertical coupled-bunch instability occurs and a broad spectrum appears for the positron beam when the threshold beam current of 9.7 mA is reached. We set the beam conditions as the total beam current of 9.8 mA with 160 bunches uniformly distributed around the storage ring in each bucket, the beam instability occurs as before. We then measure the I_c in the cases of stable and unstable beams. The results show that the relations of I_c vs. I_b and normalized I_c vs. V_b have the same regulations under the conditions of stable and unstable beams. The instability is also observed with 16.6 mA in 116 bunches, and results of I_c dependences are the same as the single bunch results. This indicates that the beam oscillation due to PEI does not influence the yield of the photoelectron.

3.5 Solenoid effect

To cure the PEI, one possible way is to use the solenoid coils winding downstream the bending magnets, like KEKB LER. In the BEPC storage ring, we installed two solenoids on each side of the PE detector to observe the effect of solenoid. The currents of the solenoid coils, I_s, are ±20A, which can generate several tens of Gauss magnetic field. Fig. 7 shows the I_c vs. I_b when solenoid has different currents. The normalized I_c when scanning the bias voltage V_b is given in Fig. 8.

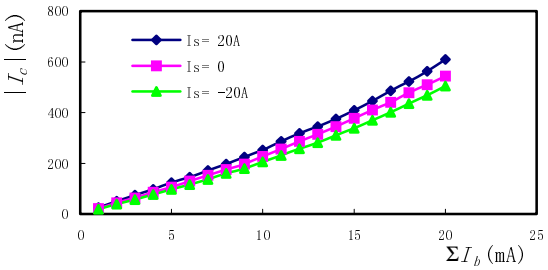

Figure 7: I_c vs. I_b with different solenoid fields.

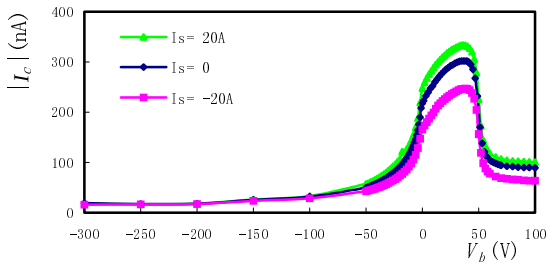

Figure 8: I_c vs. V_b with different solenoid fields.

It can be seen that the solenoid field does influence the electron cloud, but it is not a strong effect. The difference when the direction of the solenoid field changes comes from the combining effect of the solenoid field and the fringe field of the bending magnet, which is located near the detector. The combined field was also measured in the same way as the fringe field measurement described previously, resulting the fringe field and the solenoid field inside the chamber have the same order of about 10 to 30 Gauss.

4 DISCUSSIONS

Detailed measurements of the properties of PE cloud were carried out at the BEPC storage ring under various machine conditions for both stable and unstable beams. Comparisons were made between single and multi-bunch cases as well as for positron and electron beams. In most cases, the collector current, I_c, was recorded with a constant retarding voltage, V_b, of +40 V, giving the maximal signal level. For special cases, V_b was scanned from –300 V to +100 V to measure and compare the energy distribution of the electrons. It was found that I_c varies linearly with the beam current I_b as expected, since the number of photoelectrons is proportional to the photon intensity and the beam current. For positron beam I_c/I_b is ~25 nA/mA, while for electron, I_c/I_b ~5 nA/mA. This result is the same for single bunch and a number of multi-bunch patterns. There is no saturation process observed up to 40 bunches with 1 or 2 mA/bunch. We observed very weak dependence on bunch spacing, using 5 and 10 bunches with 1 to 6 mA/bunch up to the 12-bucket spacing. No beam-induced multipacting was observed at the BEPC. No significant differences were observed in I_c behaviours for stable and unstable beams.

The distance between the detector and the dipole influences the measurement of SE and saturation process very much, so in the future experiment studies, it would be very valuable to add another one or more detectors around the storage ring. The new detector should be modified as encircling the grounded grid but isolated from the retarding grid and the collector to avoid the I_c electrical leak from HOMs excited through the gap between the detector and the port. The position of the new detector should be at the straight section between two bending magnets. The time structure of I_c signal and the machine parameter dependences would be studied furthermore. Better shielding is necessary on the existing detector to avoid the fringe field of the bending magnet.

The analytical estimation and simulation are under way for more quantitative comparisons with the measurements on the total electron yield and the multipacting condition. It will be more interesting to simulate the relation of the PE properties to the PE instability, and to simulate the emittance dependence for the machine performance.

5 ACKNOWLEDGEMENTS

We wish to thank the BEPC team for their effective work on operating the machine during the experiment. The authors would also like to thank Dr. R. Rosenberg from ANL, for his suggestion on shielding the detector.

6 REFERENCES

[1] Z.Y. Guo, et al, Proceedings of PAC'97, 1997, EPAC'98, APAC'98, 1998.

[2] K.C. Harkay and R.A. Rosenberg, Proceedings of PAC'99, 1999.

[3] R.A. Rosenberg and K.C. Harkay, NIM A 453 (2000) 507.